Three-Dimensional Sheath Inked Rapid Acquisition with Refocused Echoes Imaging (SHINKEI) MRI for Delineating the Intraparotid Facial Nerve Branches and Their Anatomical Relationship with Parotid Tumors

Yanwei Jiang [1, 2], Cheng Sun [3], Wei Zhou [4], Lianpin Yu [4], Weidong Zhang [4] and Chuanting Li [1, *]

[1]Shandong Medical Imaging Research Institute Affiliated to Shandong University, Jinan, Shandong, China
[2]Binzhou People's Hospital, Binzhou, Shandong, China
[3]Binzhou Medical University Hospital, Binzhou, Shandong, China
[4]Shandong Provincial Hospital Affiliated to Shandong University, Jinan, Shandong, China

Corresponding author: Shandong Medical Imaging Research Institute Affiliated to Shandong University, 250021, China. Tel: +86-13905319867, Email: lichuanting1@126.com

Abstract

Background: Accurate imaging of the anatomical relationship between the intraparotid facial nerve branches and parotid tumor can be helpful for surgical planning and effective protection of the facial nerve during surgery. Three-dimensional sheath inked rapid acquisition with refocused echoes imaging (3D-SHINKEI) is a new MRI sequence with a high tissue contrast resolution, which has been used for imaging the peripheral nerves in several organs.

Objectives: To evaluate the value of 3D-SHINKEI sequence in representing the intraparotid facial nerve branches and their anatomical relationship with neoplasms of the parotid gland.

Patients and Methods: Thirty-six patients with parotid tumors underwent MRI with 3D-SHINKEI and 3D-T2-fast field echo (3D-T2-FFE) sequences in the coronal plane. The contrast-to-noise ratios (CNRs) and signal intensity ratios (SIRs) of the facial nerves in the two sequences were compared. The relationship between the intraparotid facial nerve branches and parotid tumor was also analyzed in 36 patients, and the results were compared with the intraoperative anatomy and postoperative pathological findings.

Results: The image quality score of the 3D-SHINKEI sequence for anatomical representation of the intraparotid facial nerve branches was significantly higher than that of the 3D-T2-FFE sequence (Z = -6.197, P < 0.01). The SIRs and CNRs of the facial nerves were significantly higher in the SHINKEI images as compared to the 3D-T2-FFE images (t = 10.772, P < 0.01 and t = 11.586, P < 0.01, respectively). The delineation accuracy of the anatomy of the main trunk of the facial nerve and its first-level branches and their relationship with tumors was significantly higher with the 3D-SHINKEI sequence than with the 3D-T2-FFE sequence (P < 0.01). Besides, the relationship between parotid tumors and the main trunk of the facial nerve and its first-level branches was classified into six types.

Conclusion: A high-resolution 3D-SHINKEI sequence could accurately represent the relationship between the intraparotid facial nerve branches and parotid gland neoplasms. It was also found to be more accurate than the 3D-T2-FFE sequence.

Keywords: Parotid Neoplasms, Facial Nerve, MRI

1. Background

The anatomical structure of the parotid gland is generally complex. It includes the main trunk of the facial nerve and its main branches (temporofacial and cervicofacial trunks), parotid ducts, and multiple blood vessels. Parotid tumors are the most common salivary gland tumors (1), which usually distort the position of these structures. Therefore, it is very important to assess their anatomical position during surgical planning (2). Magnetic resonance imaging (MRI) has been used to display the intraparotid facial nerve in some studies (3-5). However, MRI has some shortcomings. For example, the tissue contrast is poor, making distinction between the nervous and vascular structures difficult. The background signal suppression is also insufficient.

Three-dimensional sheath inked rapid acquisition with refocused echoes imaging (3D-SHINKEI) is a new sequence with a high tissue contrast resolution, in addition to fat and bloodstream signal suppression. This sequence

has been applied for imaging the peripheral nerves ([6], [7]). So far, there has been no research on the intraparotid facial nerve imaging, using the 3D-SHINKEI sequence.

2. Objectives

We aimed to evaluate the relationship between the intraparotid facial nerve and neoplasms in patients with parotid tumors using the 3D-SHINKEI sequence and to compare the results with 3D T2-fast field echo (3D T2-FFE) images and surgical findings. MRI was performed with the two sequences in the coronal plane.

3. Patients and Methods

3.1. Ethical Approval

This study was approved by the Ethics Committee of Shandong Provincial Hospital affiliated to Shandong University. All patients and healthy volunteers signed an informed consent form before examinations and data collection.

3.2. Subjects

Thirty-six patients with parotid tumors were included in this study. The patients were consecutively included based on the inclusion criteria: (1) a history of parotid tumors, confirmed pathologically; (2) undergoing MRI with 3D-SHINKEI and 3D-T2-FFE sequences; and (3) undergoing a surgical intraoperative evaluation of the facial nerve. On the other hand, the exclusion criteria were as follows: (1) severe motion artifacts in MRI; (2) facial nerve diseases, such as Bell's facial nerve paralysis; and (3) a history of parotid gland surgery or trauma.

3.3. Imaging Techniques

All examinations were conducted on a 3.0T MRI scanner (Achieva TX, Philips Healthcare, Best, the Netherlands) with an eight-channel phased-array surface coil, using 3D-SHINKEI and 3D-T2-FFE sequences. The scanning parameters of the 3D-SHINKEI sequence were as follows: (1) coronal, repetition time (TR): 2500.0 ms; (2) echo time (TE): 180.0 ms; (3) field of view (FOV): 230.0 mm × 230.0 mm; (4) voxel size: 1.0 mm × 1.0 mm × 1.0 mm; (5) matrix size: 230 × 230; section thickness: 1.0 mm; (6) slice gap: 0, 120 sections; (7) semi-acquisition factor: 0.75; (8) echo chain: 120; (9) accelerating factor: 2; (10) number of signal averages (NSA): 2; (11) improved motion-sensitized driven-equilibrium (iMSDE) preset pulse time: 50.0 ms; (12) b-value in three directions: 10 s/mm²; and (13) scanning time: 12 minutes and 13 seconds.

Moreover, the scanning parameters of the 3D-T2-FFE sequence were as follows: (1) coronal, TR: 8.7 ms; (2) TE: 3.1 ms; (3) FOV: 230.0 mm × 230.0 mm; (4) voxel size: 0.5 mm × 0.5 mm × 1.0 mm; (5) matrix size: 460 × 459, (6) section thickness: 1.0 mm; (7) section gap: 0, 70 sections; (8) NSA: 3; and (9) scanning time: 5 minutes and 14 seconds. The conventional sequences included turbo spin echo (TSE) axial T1-weighted (T1W), T2-weighted (T2W), and T2-weighted with fat suppression. The post-processing of SHINKEI and 3D-T2-FFE data included maximum intensity projection (MIP), multi-planar reconstruction (MPR), and curved multiplanar reconstruction (CPR) to better represent the intraparotid facial nerve. Through rotation and reconstruction, multi-angle and multi-directional images were constructed.

3.4. Image Analysis and Quality Control

The 3D-SHINKEI and 3D-T2-FFE images were analyzed by two radiologists with more than 20 years of experience in head and neck imaging. The facial nerve was traced from the styloid mastoid foramen. The location, course, morphology, and signal characteristics of the nerves and their relationship with tumors were delineated. If the two radiologists disagreed on a diagnosis, consensus was reached through consultation.

Based on the displayed condition of the facial nerve, the two radiologists independently scored the images in the two sequences, using a five-point scoring system. The image quality was scored according to the overall image quality, image artifacts (e.g., motion artifacts, pulsatile artifacts, and magnetic susceptibility artifacts), and signal homogeneity in the scanned areas. Generally, a score of five indicates very good to perfect quality, that is, perfect delineation of the trunk of the facial nerve and its two main branches, no noticeable artifacts, and a homogeneous signal. A score of four indicates no compromise of diagnostic quality; in other words, there are few artifacts, which do not affect the visualization of the facial nerve and its main branches, and there is a homogeneous signal with minor hyperintensities. A score of three indicates acceptable diagnostic quality, not many visible artifacts, and a homogeneous signal with major hyperintensities. A score of two indicates an unacceptable diagnostic quality; in other words, the main trunk of the facial nerve is not clearly displayed due to artifacts and an inhomogeneous signal. Finally, a score of one indicates obvious artifacts, with the main trunk of the facial nerve indistinguishable from the surrounding structures ([3]).

Moreover, the signal intensity ratio (SIR) was measured as the ratio of the signal intensity of the facial nerve to the parotid gland parenchyma in the same plane:

$$SIR = \frac{SIfn}{SIpg}$$

Where SIfn denotes the signal intensity of the intraparotid facial nerve, and SIpg is the signal intensity of the parotid gland parenchyma in the same plane. The contrast-to-noise ratio (CNR) was also calculated as follows: CNR = (SIfn- SIpg)/(SIfn + SIpg) [8].

When measuring the signal intensity of the facial nerve, the region of interest (ROI) was not placed beyond the visible length of the nerve to avoid blood vessels. Lymph nodes and artifacts were also excluded from the ROI; in the two sequences, the ROIs were carefully placed at the same location. Each ROI was 3.0 mm^2 and placed three times to obtain the mean value. The two radiologists independently analyzed the SHINKEI and 3D-T2-FFE images of the facial nerve and the anatomical relationship of this nerve and its roots with tumors. Simultaneously, the effects of benign and malignant tumors on the signal, morphology, and course of the intraparotid facial nerve were examined. The results were compared with the intraoperative anatomical findings and postoperative pathological results to assess the accuracy of these two sequences.

3.5. Statistical Analysis

SPSS 23.0® for Windows (IBM Inc., Armonk, NY, USA) was used for statistical analysis. The image score differences of the patients in the 3D-SHINKEI and 3D-T2-FFE sequences were examined by Wilcoxon signed-rank test. The SIR and CNR values were normally distributed; therefore, we compared them between the two sequences using paired sample *t*-test. Moreover, the imaging accuracy of the main trunk of the facial nerve and its first-level branches (temporofacial and cervicofacial trunks), as well as the relationship between the facial nerve and tumors, was examined using McNemar's test. P-value less than 0.05 was considered statistically significant.

4. Results

Thirty-six patients with parotid tumors were included in this study (16 males and 20 females; age range: 17 - 66 years; mean age: 43.2 ± 10.6 years). The history of parotid disease ranged from 10 days to 12 years. Overall, 32 patients had a painless parotid mass; three had a painful parotid mass; and one had bilateral parotid masses with facial nerve paralysis. All parotid tumors were confirmed by postoperative pathology, including 30 cases of benign tumors and seven cases of malignant tumors (Table 1).

Table 1. Distribution of pathological types in 36 patients with parotid tumors (37 tumors)

Postoperative Pathological Types	No. (%)
Pleomorphic adenomas (B)	19 (51.4)
Basal cell adenomas (B)	4 (10.8)
Adenolymphomas (B)	4 (10.8)
Myoepithelioma (B)	1 (2.7)
Lipoleiomyoma (B)	1 (2.7)
Hemangioma (B)	1 (2.7)
Adenoid cystic carcinoma (M)	1 (2.7)
Acinic cell carcinoma (M)	1 (2.7)
Salivary duct carcinoma (M)	1 (2.7)
Carcinoma ex pleomorphic adenoma (M)	1 (2.7)
Squamous cell carcinoma (M)	1 (2.7)
Hodgkin's lymphoma (M)	1 (2.7)
Squamous cell carcinoma on one side and adenolymphoma on the opposite side (M)	1 (2.7)
Total	37 (100)

Abbreviations: B, benign tumors; M, malignant tumors.

4.1. Image Quality of the Intraparotid Facial Nerve

The intraparotid facial nerve showed a high signal intensity in both 3D-SHINKEI and 3D-T2-FFE sequences. For both the main trunk and the first branches, the image quality score was higher with the 3D-SHINKEI sequence compared to the 3D-T2-FFE sequence. The subjective scores for the 3D-SHINKEI and 3D-T2-FFE sequences were 4.20 ± 0.55 and 3.13 ± 0.57, respectively (Z = -6.197, P < 0.001). The SIR was significantly higher with the 3D-SHINKEI sequence as compared to the 3D-T2-FFE sequence (2.23 ± 0.68 and 1.02 ± 0.20, respectively; *t* = 10.772, P < 0.001). Also, the CNR findings were similar to SIRs (Table 2).

4.2. Evaluation of the Intraparotid Facial Nerve in Patients with Parotid Tumors and Its Anatomical Relationship with Tumors

The image quality assessment results of the intraparotid facial nerve and its first-level branches in patients with parotid tumors are presented in Table 3. Compared to the intraoperative anatomical findings, there was a significant difference in the accuracy of the two sequences in representing the relationship between the main trunk of the facial nerve and its first-level branches in all 37 tumors. The accuracy was measured to be 91.9% (34/37) for the 3D-SHINKEI sequence and 51.4% (19/37) for the 3D-T2-FFE sequence (P = 0.001). The relationship between the main trunk of the facial nerve and its first-level branches and parotid tumors in the 3D-SHINKEI sequence was accurately displayed and classified into the following six types:

Table 2. Comparison of the signal intensity ratio (SIR) and contrast-to-noise ratio (CNR) of sequences in 36 patients with parotid tumors [a]

Variables	SIR	CNR
3D-SHINKEI	2.23 ± 0.68	0.59 ± 0.14
3D-T2-FFE	1.02 ± 0.20	0.28 ± 0.09
t-value	10.772	11.586
P-value	0.000	0.000

Abbreviations: 3D-SHINKEI, three-dimensional sheath inked rapid acquisition with refocused echoes imaging; 3D-T2-FFE, three-dimensional T2-fast field echo.
[a] Values are expressed as mean $\pm$ SD.

- Type 1: The location of the main trunk and first-level branches of the facial nerve did not change by parotid tumors. There were 10 cases consistent with this type on the 3D-SHINKEI images.

- Type 2: The temporofacial trunk was compressed by a parotid tumor, and its position was changed. Images of eight patients were categorized in this group.

- Type 3: The cervicofacial trunk was compressed by a tumor, which changed its anatomy. Five cases belonged to this category.

- Type 4: Both of the main first-level branches of the facial nerve (temporofacial and cervicofacial trunks) were compressed by a parotid tumor, and their positions were changed. This anatomical relationship was determined in three patients.

- Type 5: The main trunk and first-level branches of the facial nerve were surrounded by a parotid tumor, as found in four patients (Figure 1).

- Type 6: The main trunk and first-level branches of the facial nerve were invaded by a parotid tumor, as found in four patients (Figure 2).

Three lesions were affected by artifacts or the large size of tumors, obliterating the anatomical relationship with the facial nerve on 3D-SHINKEI images. Unlike benign parotid tumors, malignant parotid tumors can invade the facial nerve. The main trunk and first-level branches of the facial nerve changed in type 6 tumors due to tumor infiltration. The 3D-SHINKEI images of four patients with malignant tumors were characterized by a thickening diameter, signal enhancement, and non-uniformity of the main trunk and first-level branches (Figure 2); in one case, only the first-level branches of the facial nerve were involved.

5. Discussion

Knowledge of the anatomy of the facial nerve in the parotid gland can be helpful in surgical planning. Different strongly T2- or T2*-weighted volume 3D MRI sequences have been advocated for evaluating the peripheral nerves, including 3D gradient-recalled acquisition in steady state (3D-GRASS), 3D constructive interference in steady state (3D-CISS), and 3D fast imaging employing steady-state acquisition (3D-FIESTA) (9-11). The peripheral nerves showed a low signal intensity, while the cerebrospinal fluid showed a high signal intensity in these sequences. Therefore, the main trunk of the facial nerve and its main branches (temporofacial and cervicofacial trunks) were not surrounded by a fluid material, resulting in the insufficient signal contrast of the image. The facial nerve branches in the parotid gland parenchyma were particularly thin in diameter, and it was difficult to distinguish them from the peripheral vascular signals.

Because diffusion-weighted imaging (DWI) exerts an inhibitory effect on signals from the peripheral fat and blood flow, the sequences generated by DWI and T2WI may better show the anatomy and lesions of peripheral nerves. Today, the most studied sequence is 3D fast imaging with steady-state precession and diffusion-weighted imaging (3D-PSIF-DWI). Studies on healthy volunteers show that the intraparotid facial nerve is well displayed by this sequence (5). However, the theoretical composition of the sequence was complex, and imaging was very difficult; also, this study was limited to healthy volunteers.

The 3D-SHINKEI sequence can visualize the nerve sheath due to the reduction of signals from fat, vessels, and muscles. The present findings showed that the image quality score of the intraparotid facial nerve in the 3D-SHINKEI sequence was higher than that of the 3D-T2-FFE sequence in healthy volunteers. The accuracy of representing the relationship between the main trunk of the facial nerve and the main first-level branches in the 3D-SHINKEI sequence was higher than the 3D-T2-FFE sequence. The relationship between the main trunk of the facial nerve and the main first-level branches in parotid tumors was classified into six types.

The 3D-SHINKEI sequence is a 3D-TSE sequence in combination with short tau inversion recovery (STIR) and iMSDE pulse. The main function of the iMSDE preset pulse is to inhibit the blood flow signals in vessels accompanying the nerve, as it can inhibit the blood flow signals in any direction, especially for perfusion and eddy current liquid signals (12, 13). In this way, the fat, blood flow, muscle, and
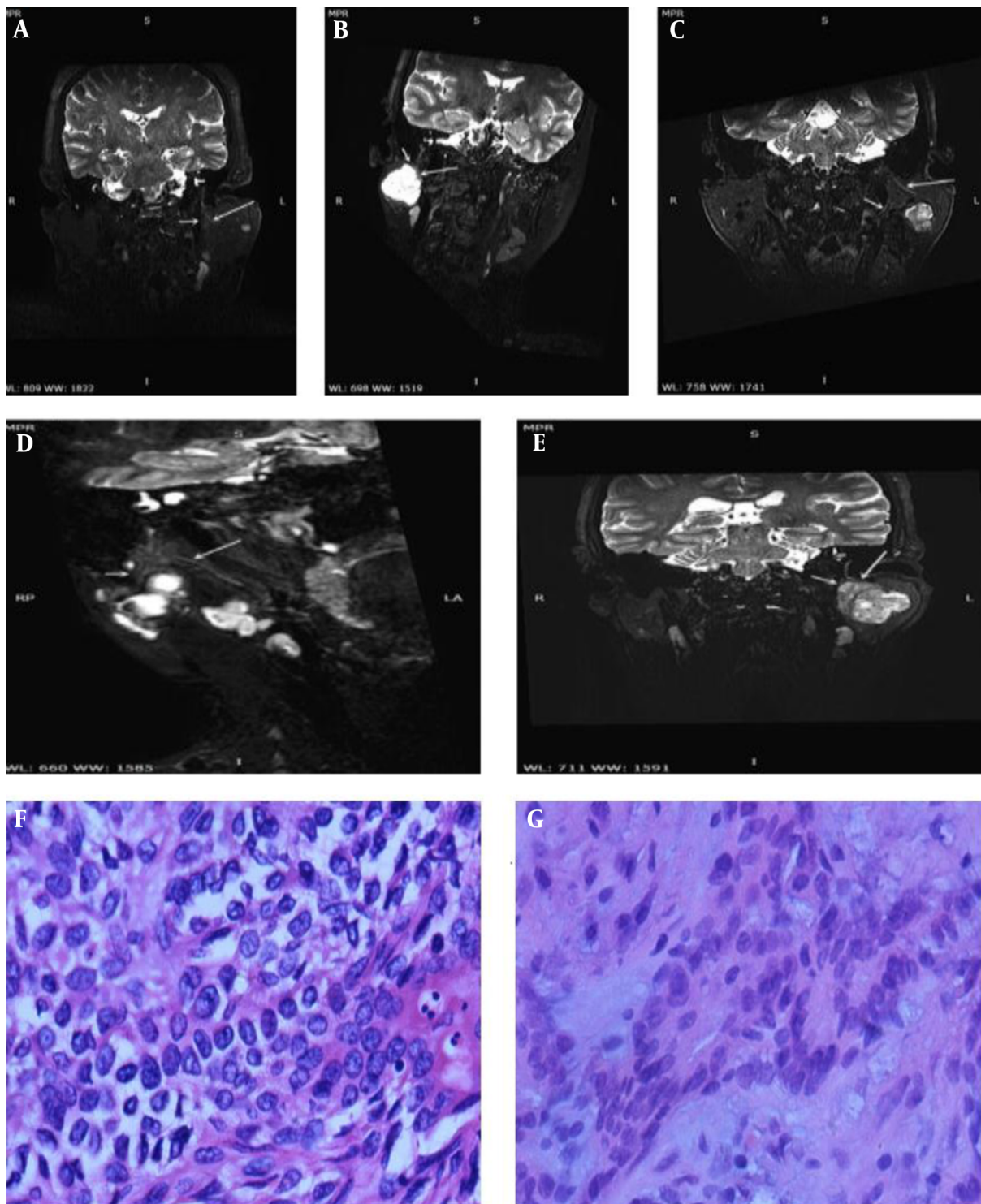
Jiang Y et al.

Figure 1. (A) A 54-year-old woman with basal cell adenoma; (B) a 26-year-old woman with pleomorphic adenoma; (C) a 66-year-old man with pleomorphic adenoma; (D) a 28-year-old woman with pleomorphic adenoma; and (E) a 38-year-old man with pleomorphic adenoma. The relationships between the main trunk of the facial nerve and its first-level branches with tumors are shown successively in post-reconstruction 3D-SHINKEI sequence images (arrow); and (F & G) histopathology of pleomorphic adenoma and basal cell adenoma (hematoxylin-eosin staining, ×400).

Table 3. Comparison of the visibility of the main trunk and first-level branches of the facial nerve between the two sequences in 36 patients with parotid gland tumors (37 tumors) [a]

Variables	Main Trunk of the Facial Nerve (37)	Temporofacial Trunk (37)	Cervicofacial Trunk (37)
3D-SHINKEI	37 (100)	34 (91.2)	35 (94.6)
3D-T2-FFE	35 (94.6)	19 (51.4)	24 (64.9)
P-value	0.782	0.001	0.014

[a] Values are expressed as No. (%).
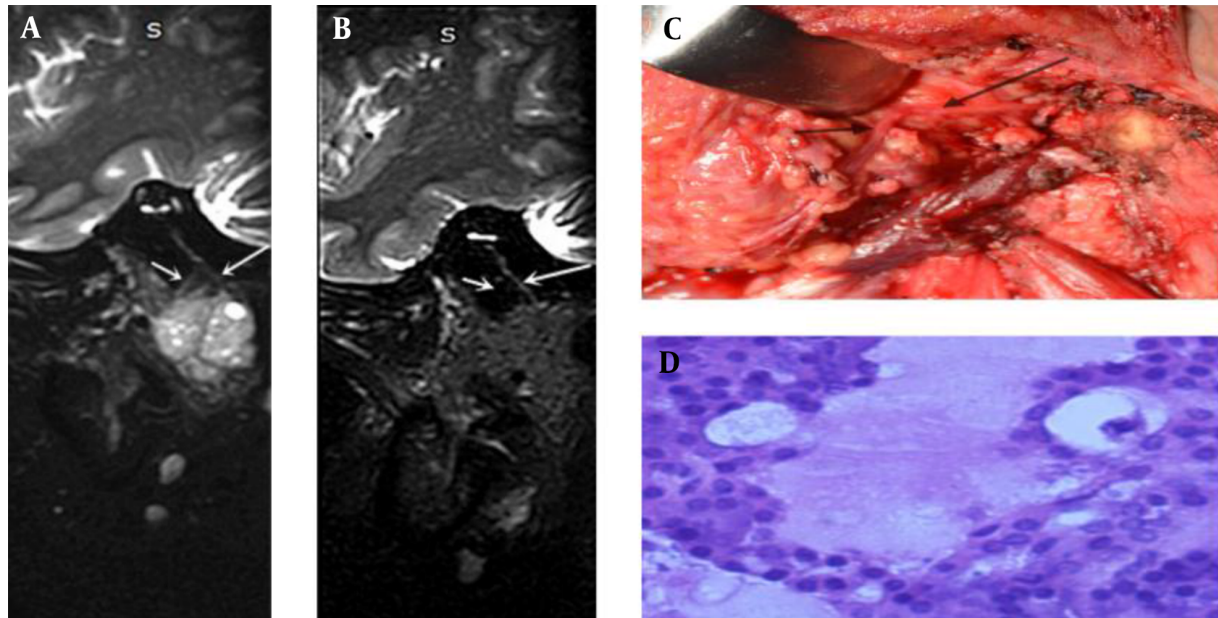
Figure 2. A 29-year-old woman with acinic cell carcinoma: (A) tumor side and (B) healthy side. Both the main trunk of the facial nerve and first-level branches (long arrow: cervicofacial trunk; short arrow: temporofacial trunk) on the tumor side are thicker than the healthy side; (C) intraoperative anatomy; and (D) histopathology (hematoxylin-eosin staining, ×400).

other soft tissue signals in the area of the parotid gland are suppressed to the greatest extent, and the nerve signals become more prominent.

The iMSDE has been shown to improve the visualization of nerves in different anatomical regions. In a previous study, the brachial plexus, lumbosacral plexus, and trigeminal nerve of five healthy volunteers were displayed clearly with the iMSDE sequence (8). Researchers have also suggested this MRI sequence for the lumbosacral plexus in case of chronic neuropathy (7, 14). Visual evaluation of the celiac plexus can be achieved using respiratory- and cardiac-triggered 3D-SHINKEI-magnetic resonance neurography (MRN) (15).

In terms of scanning time alone, the 3D-T2-FFE sequence was significantly shorter than the 3D-SHINKEI sequence. Our results showed that both SIR and CNR were higher on the SHINKEI sequence compared to the 3D-T2-FFE sequence. The image quality score of the SHINKEI se-

quence was also higher than that of 3D-T2-FFE, indicating a significantly better image quality. In visualization of the main trunk of the facial nerve, there were insignificant differences between the 3D-SHINKEI and 3D-T2-FFE sequences. However, for the temporofacial and cervicofacial trunks, the 3D-SHINKEI sequence showed obvious advantages. According to the mentioned results, the main trunk of the facial nerve and its first-level branches were related to the location of benign tumors (in five types). The 3D-SHINKEI images were superior to 3D-T2-FFE images in terms of signal strength and signal uniformity. Overall, 3D-SHINKEI showed significant advantages in indicating the anatomical relationship between the intraparotid facial nerve and tumors.

In a normal parotid gland, the intraparotid facial nerve, parotid ducts, and blood vessels have relatively fixed positions. If tumors develop in the parotid gland, their position may change. Once a tumor grows in the parotid

gland, its position and shape will transform due to the squeezing and invasion of the tumor. Surgery is the most important treatment for the parotid gland tumors. Therefore, accurate imaging of the intraparotid facial nerve in surgical planning is particularly important for the effective protection of the facial nerve during surgery. Overall, the 3D-SHINKEI sequence can display the relationship between the tumor and the intraparotid facial nerve position before surgery. It is also helpful in protecting the facial nerve during surgery, facilitating the functional recovery of the facial nerve after surgery, and improving the patient's quality of life.

Among 36 patients with parotid gland tumors, seven had malignant tumors. An important feature of a parotid gland malignancy is invasion to the facial nerve (16). In 3D-SHINKEI images of all seven patients with malignant tumors, four showed type 5 and 6 involvement; involvement of the main trunk and/or its first-level branches showed thickening, signal enhancement, and non-uniformity. Although removal of the intraparotid facial nerve is essential in malignant parotid tumors, inappropriate intraparotid facial nerve removal can be harmful, causing many problems for the patient. Suspicion of the intraparotid facial nerve invasion can be shown by 3D-SHINKEI images, and the surgeon can preoperatively inform the patient of the risk of intraoperative removal and subsequent loss of function. However, there is no literature on the signs of facial nerve changes in parotid gland malignant tumors using 3D-SHINKEI.

The present study had several limitations. First, the 3D-SHINKEI scanning time is long, and patient compliance is not simple. Second, the number of patients was small, and the pathological types were incomplete, especially in patients with malignant tumors. Third, the 3D-iMSDE sequence was not ideal for imaging the secondary branches of the intraparotid facial nerve. Finally, due to differences in the anatomical route, the tumor and the intraparotid facial nerve could not always be fully visualized together in one plane despite postprocessing; further research is needed to improve and overcome these problems.

In conclusion, the 3D-SHINKEI-MRN sequence has high spatial resolution, CNR, and SIR for the intraparotid facial nerve and the main first-level branches and can clearly show the relationship between the nerves and a parotid gland tumor. It is suggested to optimize the facial nerve protection in preoperative planning and guide the postoperative rehabilitation treatment plans. We recommend this sequence for the MRI examination of patients with parotid gland tumors.

Footnotes

References

1. Kanatas A, Ho MWS, Mucke T. Current thinking about the management of recurrent pleomorphic adenoma of the parotid: A structured review. *Br J Oral Maxillofac Surg.* 2018;**56**(4):243–8. doi: 10.1016/j.bjoms.2018.01.021. [PubMed: 29526342].

2. Eski E, Sokmen MF, Yilmaz I. Segmental superficial parotidectomy in the surgical treatment of benign parotid tumours. *J Laryngol Otol.* 2018;**132**(4):356–9. doi: 10.1017/S0022215118000245. [PubMed: 29463342].

3. Zhao Y, Yang B. Value of visualization of the intraparotid facial nerve and parotid duct using a micro surface coil and three-dimensional reversed fast imaging with steady-state precession and diffusion-weighted imaging sequence. *J Craniofac Surg.* 2018;**29**(8):e754–7. doi: 10.1097/SCS.0000000000004704. [PubMed: 29927823].

4. Attye A, Karkas A, Tropres I, Roustit M, Kastler A, Bettega G, et al. Parotid gland tumours: MR tractography to assess contact with the facial nerve. *Eur Radiol.* 2016;**26**(7):2233–41. doi: 10.1007/s00330-015-4049-9. [PubMed: 26449562].

5. Chu J, Zhou Z, Hong G, Guan J, Li S, Rao L, et al. High-resolution MRI of the intraparotid facial nerve based on a microsurface coil and a 3D reversed fast imaging with steady-state precession DWI sequence at 3T. *AJNR Am J Neuroradiol.* 2013;**34**(8):1643–8. doi: 10.3174/ajnr.A3472. [PubMed: 23578676]. [PubMed Central: PMC8051441].

6. Hiwatashi A, Togao O, Yamashita K, Kikuchi K, Ogata H, Yamasaki R, et al. Evaluation of chronic inflammatory demyelinating polyneuropathy: 3D nerve-sheath signal increased with inked rest-tissue rapid acquisition of relaxation enhancement imaging (3D SHINKEI). *Eur Radiol.* 2017;**27**(2):447–53. doi: 10.1007/s00330-016-4406-3. [PubMed: 27208993].

7. Kasper JM, Wadhwa V, Scott KM, Rozen S, Xi Y, Chhabra A. SHINKEI–a novel 3D isotropic MR neurography technique: technical advantages over 3DIRTSE-based imaging. *Eur Radiol.* 2015;**25**(6):1672–7. doi: 10.1007/s00330-014-3552-8. [PubMed: 25638217].

8. Yoneyama M, Takahara T, Kwee TC, Nakamura M, Tabuchi T. Rapid high resolution MR neurography with a diffusion-weighted pre-pulse. *Magn Reson Med Sci.* 2013;**12**(2):111–9. doi: 10.2463/mrms.2012-0063. [PubMed: 23666153].

9. Dailiana T, Chakeres D, Schmalbrock P, Williams P, Aletras A. High-resolution MR of the intraparotid facial nerve and parotid duct. *AJNR Am J Neuroradiol*. 1997;**18**(1):165–72. [PubMed: 9010536]. [PubMed Central: PMC8337863].

10. Takahashi N, Okamoto K, Ohkubo M, Kawana M. High-resolution magnetic resonance of the extracranial facial nerve and parotid duct: Demonstration of the branches of the intraparotid facial nerve and its relation to parotid tumours by MRI with a surface coil. *Clin Radiol*. 2005;**60**(3):349–54. doi: 10.1016/j.crad.2004.06.018. [PubMed: 15710138].

11. Li C, Li Y, Zhang D, Yang Z, Wu L. 3D-FIESTA MRI at 3 T demonstrating branches of the intraparotid facial nerve, parotid ducts and relation with benign parotid tumours. *Clin Radiol*. 2012;**67**(11):1078–82. doi: 10.1016/j.crad.2012.03.014. [PubMed: 22608246].

12. Choi JW, Han M, Hong JM, Lee JS, Kim SY, Kim SS. Feasibility of improved motion-sensitized driven-equilibrium (iMSDE) prepared 3D T1-weighted imaging in the diagnosis of vertebrobasilar artery dissection. *J Neuroradiol*. 2018;**45**(3):186–91. doi: 10.1016/j.neurad.2017.11.006. [PubMed: 29273530].

13. Obara M, Kuroda K, Wang J, Honda M, Yoneyama M, Imai Y, et al. Comparison between two types of improved motion-sensitized driven-equilibrium (iMSDE) for intracranial black-blood imaging at 3.0 tesla. *J Magn Reson Imaging*. 2014;**40**(4):824–31. doi: 10.1002/jmri.24430. [PubMed: 24924316].

14. Hiwatashi A, Togao O, Yamashita K, Kikuchi K, Momosaka D, Nakatake H, et al. Lumbar plexus in patients with chronic inflammatory demyelinating polyradiculoneuropathy: evaluation with simultaneous T2 mapping and neurography method with SHINKEI. *Br J Radiol*. 2018;**91**(1092):20180501. doi: 10.1259/bjr.20180501. [PubMed: 30160180]. [PubMed Central: PMC6319828].

15. Ferrer CJ, Bos C, Yoneyama M, Obara M, Kok L, van Leeuwen MS, et al. Respiratory- and cardiac-triggered three-dimensional sheath inked rapid acquisition with refocused echoes imaging (SHINKEI) of the abdomen for magnetic resonance neurography of the celiac plexus. *Eur Radiol Exp*. 2019;**3**(1):14. doi: 10.1186/s41747-019-0095-4. [PubMed: 30923930]. [PubMed Central: PMC6439132].

16. Guntinas-Lichius O, Silver CE, Thielker J, Bernal-Sprekelsen M, Bradford CR, De Bree R, et al. Management of the facial nerve in parotid cancer: Preservation or resection and reconstruction. *Eur Arch Otorhinolaryngol*. 2018;**275**(11):2615–26. doi: 10.1007/s00405-018-5154-6. [PubMed: 30267218].